JACC: CARDIOVASCULAR IMAGING
VOL. 4, NO. 6, 2011
© 2011 BY THE AMERICAN COLLEGE OF CARDIOLOGY FOUNDATION
ISSN 1936-878X/$36.00
PUBLISHED BY ELSEVIER INC.
DOI:10.1016/j.jcmg.2011.03.015

CVN Interview

Peri-Infarct Zone on Early Contrast-Enhanced CMR Imaging in Patients With Acute Myocardial Infarction

Hidenari Matsumoto, MD, PHD,* Tetsuya Matsuda, MD, PHD,† Kenichi Miyamoto, RT,‡ Toshihiko Shimada, MD, PHD,§ Mikiko Mikuri, MD,* Yuji Hiraoka, MD, PHD*

Kyoto, Japan

OBJECTIVES The aims of this study were to evaluate hyperenhanced regions on contrast-enhanced cardiovascular magnetic resonance (CE-CMR) imaging in patients with acute myocardial infarction (AMI) between early contrast-enhanced cardiovascular magnetic resonance (ECE) (2 min) and late contrast-enhanced cardiovascular magnetic resonance (LCE) (10 to 15 min) after gadolinium administration, and to compare the CE-CMR images with area at risk (AAR) derived from T2-weighted (T2W) CMR.

BACKGROUND Although CE-CMR imaging can demarcate the infarcted myocardium, the value of hyperenhancement in AMI is still in dispute. The size of hyperenhanced regions may vary with time, and overestimation can be often observed with early acquisition.

METHODS Thirty-four patients with successfully reperfused AMI underwent CMR within 4 days after the event. Myocardial regions as percentage of left ventricular (LV) myocardium were quantified on CE and T2W images. Relative peri-infarct zone was calculated as the difference in hyperenhanced regions between ECE and LCE, normalized to the individual infarct size.

RESULTS Both ECE and LCE images revealed hyperenhancement in the territory of the infarct-related artery in all patients. The hyperenhanced region on ECE extended transmurally and was consistently larger than that on LCE (39 ± 12% vs. 27 ± 12% of LV myocardium, $p < 0.001$). The relative peri-infarct zone was inversely correlated with the transmurality of infarction ($r = -0.59$, $p < 0.001$) and the time from symptom to reperfusion ($r = -0.46$, $p < 0.01$). The hyperenhanced region on ECE was correlated with the T2W CMR-derived AAR ($r = 0.86$, $p < 0.001$) with the average difference of −0.8% and the limits of agreement of ±11.9%.

CONCLUSIONS ECE depicts ischemically injured but salvaged myocardium, as well as infarcted myocardium in patients with AMI. The myocardium at risk and infarcted myocardium after reperfusion can be retrospectively assessed by the combination of ECE and LCE. (J Am Coll Cardiol Img 2011;4: 610–8) © 2011 by the American College of Cardiology Foundation

From the *Cardiovascular Center, Rakuwakai Otowa Hospital, Kyoto, Japan; †Department of Systems Science, Kyoto University Graduate School of Informatics, Kyoto, Japan; ‡Department of Radiological Technology, Rakuwakai Otowa Hospital, Kyoto, Japan; and the §Department of General Internal Medicine, Rakuwakai Otowa Hospital, Kyoto, Japan. The authors have reported that they have no relationships to disclose.

Manuscript received January 16, 2011; revised manuscript received March 3, 2011, accepted March 14, 2011.

In the setting of acute myocardial infarction (AMI), the identification of viable or nonviable myocardium is important for patient management. Contrast-enhanced (CE) cardiac magnetic resonance (CMR) imaging has been well established for visualizing both acute and chronic myocardial infarction (1,2). The mechanism for myocardial tissue enhancement with a gadolinium-based contrast agent is related to an altered sarcolemmal membrane integrity in the acute setting (3). However, the value of hyperenhancement early after injury remains to be completely elucidated because of a complex healing process.

See page 619

Hyperenhanced regions in AMI are independent of post-contrast imaging time between 5 and 40 min when the inversion time (TI) is adjusted (4), and myocardial injury without necrosis due to transient ischemia does not lead to hyperenhancement despite the presence of myocardial stunning (5). On the other hand, several reports have indicated that the enhanced region encompasses not only the nonviable myocardium, but also the reversibly injured myocardium (6–9). The size of hyperenhanced regions may vary with time after gadolinium injection, and overestimation can be particularly observed with early acquisition (10,11). Therefore, the hyperenhanced regions early after gadolinium administration in the setting of AMI could include salvaged myocardium.

Thus far, CE images obtained early after contrast administration using the current standard technique have not, to our knowledge, been studied. We hypothesized that early CE imaging demarcates the area at risk (AAR) in patients with AMI. In this study, CE imaging within 4 days after the event was conducted at 2 min (early contrast-enhanced cardiac magnetic resonance [ECE]) and 10 to 15 min (late contrast-enhanced cardiac magnetic resonance [LCE]) after gadolinium administration. The aims of this study were to evaluate the hyperenhanced regions between 2 sets of CE images in patients with reperfused AMI, and to compare the ECE images with AAR derived from T2-weighted (T2W) CMR images (12–14).

METHODS

The study protocol was approved by the local ethics committee, and written informed consent was obtained from all patients before the examination.

Study patients. Our prospective study enrolled 34 consecutive patients who experienced their first AMI with total or subtotal coronary artery occlusion and subsequently underwent primary percutaneous coronary intervention within 2 days after the onset of symptoms. Percutaneous coronary intervention was performed immediately after hospital admission in all patients. The CMR study was carried out within 4 days after the onset of symptoms. The diagnosis of AMI was based on clinical history of persistent typical chest pain, characteristic electrocardiographic changes, and rise of cardiac biomarkers. Exclusion criteria included primary myocardial disease, unstable hemodynamic state, inability to hold a breath during scanning, severe arrhythmia, or any contraindications for CE-CMR examination.

CMR imaging protocol. Imaging was performed on a 1.5-T scanner (MAGNETOM Avanto, Siemens Healthcare, Erlangen, Germany) with a 12-channel phased-array coil, electrocardiogram gating, and breath-holding condition. Images were acquired in 3 standard short-axis slices (basal, midventricular, and apical), which were kept identical for each sequence throughout the CMR examination (14).

For AAR determination, a T2W triple inversion recovery turbo spin echo sequence was employed with the following parameters: repetition time/echo time, 2 heartbeats/64 ms; TI, 140 ms; echo-train length, 17; GRAPPA factor, 2; and typical spatial resolution, 1.9 × 1.3 × 15 mm. A bolus of 0.15 mmol/kg gadolinium-based contrast agent (meglumine gadoterate; Magnescope, Guerbet, Villepinte, France) was administered with a mechanical injector at 4 ml/s, followed by a 25-ml saline flush. ECE and LCE images were acquired 2 min and 10 to 15 min after gadolinium administration, respectively. CE imaging was performed using a segmented inversion-recovery gradient-echo sequence with the following parameters: repetition time/echo time, 7.1 ms/3.3 ms; flip angle, 25°; TI determined to null normal myocardium, GRAPPA factor, 2; and typical spatial resolution, 2.0 × 1.4 × 15 mm. Just before each CE imaging, a segmented inversion recovery steady-state free-precession pulse sequence (TI scout) acquisition was performed to determine the optimal TI.

Image analysis. Offline image analysis was performed with dedicated software by the consensus of

ABBREVIATIONS AND ACRONYMS

AAR = area at risk
AMI = acute myocardial infarction
CE = contrast-enhanced
CMR = cardiac magnetic resonance
ECE = early contrast-enhanced cardiac magnetic resonance
LCE = late contrast-enhanced cardiac magnetic resonance
LV = left ventricle/ventricular
TI = inversion time
TIMI = Thrombolysis In Myocardial Infarction
T2W = T2-weighted

JACC: CARDIOVASCULAR IMAGING, VOL. 4, NO. 6, 2011
JUNE 2011:610–8

2 experienced observers (H.M. and T.M.), who were blinded regarding the patients' clinical data. Endocardial and epicardial contours were traced manually. Once the myocardial contours were identified, myocardial regions were delineated manually for CE and T2W images. Regions with a hypointense signal within the area with increased signal intensity on T2W images and hypoenhanced regions within hyperenhanced myocardium on CE images were included in the myocardial region. Myocardial regions were expressed as a percentage of total left ventricular (LV) volumes. The relative peri-infarct zone was calculated as the difference in hyperenhanced regions between ECE and LCE, normalized to the individual infarct size. Using a 17-segment model (except for segment 17) (15), the transmural extent of hyperenhancement was visually assessed with a 5-point scale (0, no hyperenhancement; 1, 1% to 25%; 2, 26% to 50%; 3, 51% to 75%; 4, 76% to 100%) (1). The mean transmurality score was calculated as the sum of all segmental scores divided by the number of segments with hyperenhancement.

In 1 representative short-axis slice in which the peri-infarct zone on ECE was greatest, quantitative analysis was performed. In CE images, regions of interest (>20 mm^2) were placed within the peri-infarct zone and the remote myocardium to measure the mean signal intensity. The standard deviation of background noise (σ) was also measured outside the body. The region of interest in each region was placed in approximately the same location and size in T2W images as well. Signal-to-noise ratio and contrast-to-noise ratio were calculated as the following equations: signal-to-noise ratio = mean signal intensity of peri-infarct/σ; contrast-to-noise ratio = (mean signal intensity of peri-infarct − mean signal intensity of remote)/σ, respectively. However, signal-to-noise ratio and contrast-to-noise ratio should be considered only as approximations in the setting of parallel imaging. Seven patients were excluded from quantitative analysis because the peri-infarct zone was so small that regions of interest could not be placed.

Statistical analysis. Statistical analysis was performed with PASW Statistics 18 (SPSS Inc., Chicago, Illinois). Quantitative variables were expressed as mean ± SD or median (25th, 75th percentile), depending on distribution. Categorical variables were expressed as frequencies or percentages. Comparisons of quantitative variables were done with a paired *t* test or Wilcoxon signed rank test. Mann-Whitney *U* test was used for comparing relative peri-infarct zone between the groups of subjects. Correlation between the T2W CMR-derived AAR and the hyperenhanced region on ECE was assessed with the use of Pearson correlation coefficient. Other correlations between continuous variables were assessed using Spearman rank correlation coefficient. The agreement between the T2W CMR-derived AAR and the hyperenhanced region on ECE was examined using Bland-Altman analysis. A p value <0.05 was considered a statistically significant difference.

RESULTS

Patient characteristics and clinical results. Patient characteristics are shown in Table 1. Primary PCI was successfully performed in all the patients. Stents were implanted in 32 patients (94%), and thrombolysis was not performed. There were no clinical events suggesting reocclusion or stenosis in the period between reperfusion therapy and CMR examination.

Visual segmental analysis of hyperenhancement. In all patients, the hyperenhanced regions were observed in the territory of the infarct-related artery on both ECE and LCE images. Table 2 sums up the comparison of the transmural extent between ECE and LCE on a regional basis. Of the 544 segments, 201 on ECE and 190 on LCE had hyperenhancement. The hyperenhancement on ECE was transmural in most of the involved segments. Fifteen segments with hyperenhancement on ECE had none on LCE. Although 4 segments with hyperenhancement on LCE were assigned to grade 0 on ECE, this difference was

Table 1. Patient Characteristics (n = 34)

Age, yrs	67 ± 10
Male/female	22/12
Time from symptom onset to reperfusion, h	3.9 (2.7, 8.5)
Time from symptom onset to CMR, h	62.3 ± 20.5
Time from reperfusion to CMR, h	52.4 ± 19.3
ST-segment elevation myocardial infarction	31 (91)
Angiographic data	
Culprit location (LAD/LCX/RCA)	15/7/12
Number of diseased vessels (1/2/3)	25/6/2
TIMI grade before reperfusion (0/1/2/3)	16/5/10/3
TIMI grade after reperfusion (0/1/2/3)	0/0/7/27
Collateral grade (0/1/2/3)	7/17/9/1

Values are expressed as n, mean ± SD, n (%), or median (25th, 75th percentile).
CMR = cardiac magnetic resonance; LAD = left anterior descending coronary artery; LCX = left circumflex coronary artery; RCA = right coronary artery; TIMI = Thrombolysis In Myocardial Infarction.

due to a different assignment of the 17-segment model. Of the 190 segments with hyperenhancement on LCE, 96 (51%) had comparable and 89 (47%) had greater transmural extent of hyperenhancement on ECE. The mean transmurality score of ECE was significantly greater than that of LCE (transmurality score: 3.9 [3.7, 4.0] vs. 3.2 [2.8, 3.8], $p < 0.001$).

Peri-infarct zone on ECE. The hyperenhanced region on ECE was consistently larger than that on LCE (Fig. 1) and exceeded by 12 ± 10% (39 ± 12% vs. 27 ± 12% of LV myocardium, $p < 0.001$). The relative peri-infarct zone normalized to infarct size on ECE was 37% (19%, 72%). As shown in Figure 2, the relative peri-infarct zone was correlated inversely with the mean transmurality score on LCE ($r = -0.59$, $p < 0.001$). This finding indicated that subendocardial infarcts revealed a larger peri-infarct zone on ECE compared with transmural infarcts. Representative images are shown in Figure 3.

An inverse relationship was found between the relative peri-infarct zone and the time from symptom to reperfusion ($r = -0.46$, $p < 0.01$). When separating the subjects into 2 subgroups based upon the median time from symptom to reperfusion (3.9 h), the group with early reperfusion had larger relative peri-infarction zone than the group with late reperfusion (57% [27%, 140%] vs. 27% [11%, 42%], $p < 0.05$). No significant relationship was found between the relative peri-infarct zone and the time from reperfusion to CMR ($r = 0.08$, $p = 0.67$). The subjects with Thrombolysis In Myocardial Infarction (TIMI) flow grade 3 after reperfusion tended to have a larger relative peri-infarct zone in comparison with those with TIMI flow grade ≤2 (37% [22%, 76%] vs. 20% [4%, 43%], $p = 0.09$). There was no significant difference in relative peri-infarction zone between groups with or without good collaterals (grade ≥2) (42% [14%, 106%] vs. 35% [21%, 64%], $p = 0.65$).

Hyperenhancement on ECE versus T2W CMR-derived AAR. In all patients, the location of increased signal intensity areas in T2W images corresponded to the territory of infarct-related artery. The T2W CMR-derived AAR ranged from 16% to 58% of LV myocardium (mean, 38% ± 10%) and was significantly larger than the hyperenhanced region on LCE ($p < 0.001$). Meanwhile, there was a significant correlation between the T2W CMR-derived AAR and the hyperenhanced region on ECE ($r = 0.86$, $p < 0.001$) (Fig. 4A). Figure 4B shows the results of Bland-Altman analysis of the difference between the T2W CMR-derived AAR and the hyperenhanced region on ECE. The average difference (bias) was −0.8% of LV myocardium, and the limits of agreement were −12.8% and 11.1% of LV myocardium.

In the peri-infarct zone, the contrast-to-noise ratio on ECE was not significantly different from T2W CMR (19 [16, 26] vs. 15 [7, 22], $p = 0.06$), whereas the signal-to-noise ratio on ECE was significantly lower than on T2W CMR (25 [20, 31] vs. 65 [54, 84], $p < 0.001$). The difference in the signal-to-noise ratio could be related to the inher-

Table 2. Comparison of Transmural Extent of Hyperenhancement Between ECE and LCE on a Regional Basis

	LCE					
ECE	**0%**	**1%–25%**	**26%–50%**	**51%–75%**	**76%–100%**	**Total**
0%	339	1	0	1	2	343
1%–25%	0	0	0	0	0	0
26%–50%	0	0	2	0	0	2
51%–75%	3	3	12	5	1	24
76%–100%	12	5	19	50	89	175
Total	354	9	33	56	92	544

ECE = early contrast-enhanced cardiac magnetic resonance imaging; LCE = late contrast-enhanced cardiac magnetic resonance imaging.

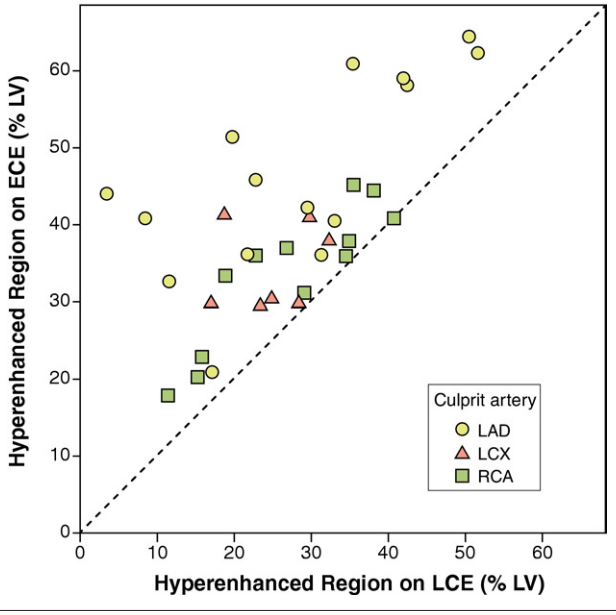

Figure 1. Hyperenhanced Region on ECE and LCE

Hyperenhanced region as percentage of left ventricular (LV) myocardium on early contrast-enhanced cardiac magnetic resonance imaging (ECE) was consistently greater than that on late contrast-enhanced cardiac magnetic resonance imaging (LCE). The **dashed line** indicates the line of identity. LAD = left anterior descending coronary artery; LCX = left circumflex coronary artery; RCA = right coronary artery.

JACC: CARDIOVASCULAR IMAGING, VOL. 4, NO. 6, 2011
JUNE 2011:610–8

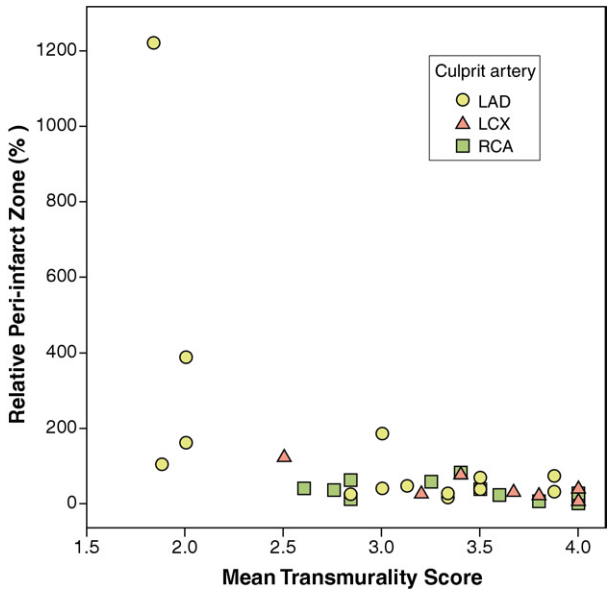

Figure 2. Peri-Infarct Zone and Transmurality of Infarct

Inverse correlation between size of the relative peri-infarct zone on ECE, normalized to infarct size, and the mean transmurality score on LCE ($r = -0.59$, $p < 0.001$). Abbreviations as in Figure 1.

ent characteristics of sequences (gradient-echo sequence vs. spin echo sequence).

DISCUSSION

ECE depicted the hyperenhanced region in the territory of infarct-related artery in all patients with reperfused AMI within 4 days after the event. The hyperenhanced region on ECE extended transmurally and was consistently larger than that on LCE. Moreover, the percentage area of hyperenhancement on ECE was correlated with the T2W CMR-derived AAR regardless of transmurality of infarction. Our data suggests that ECE demarcates not only the region of infarct, but also the peri-infarct region, which is injured by ischemia but remains viable.

Peri-infarct zone on ECE. Mechanisms of hyperenhancement in AMI is still in dispute since the myocardium undergoes a complex healing process consisting of edema, inflammation, and replacement of necrotic cardiomyocytes. In the setting of AMI, the size of hyperenhanced regions on CE imaging is reported as being overestimated compared with the true infarct size (6–9). Although it is presumed that the overestimations could be attributable to older CMR techniques (3) or an incorrect TI (16), our findings using the current standard CMR technique and the adjusted TI suggest that the hyperenhanced regions on ECE include salvaged myocardium surrounding the acute infarct. The segmented inversion-recovery gradient-echo sequence used for CE imaging in the present study, which has strong T1 weighting and low T2 sensitivity, supports the conclusion that hyperenhancement in the peri-infarct zone on ECE is gadolinium-related.

Even in successful early revascularization, intermittent coronary artery occlusion affects the entire perfusion bed. Ischemic but viable peri-infarct zone undergoes changes in osmotic colloidal pressure due to the leakage of plasma proteins (17) and/or the degradation of the extracellular matrix (18). Arheden et al. (19) found a difference in the fractional distribution volume of gadolinium among acutely infarcted myocardium, peri-infarct zone, and normal myocardium. The distribution volume in the peri-infarct zone was at the level intermediate between infarcted and normal myocardium, and increased significantly with prolongation of ischemic period. Hence, the T1 value in the peri-infarct zone would be shorter than that in normal myocardium regardless of imaging time after gadolinium administration. Although constant partition coefficients were found throughout gadolinium clearance for both normal and acutely injured myocardium in rats (19), the partition coefficient in acutely infarcted myocardium changed over time in a human study, which indicated altered wash-in and washout kinetics of gadolinium (20). Although human gadolinium kinetics in the peri-infarct zone has yet to be fully elucidated, the difference in gadolinium kinetics between the peri-infarct zone and normal myocardium could be attributed to the fading of hyperenhancement in the peri-infarct zone on LCE.

On the other hand, several discrepant reports have been previously published (3,21). Rehwald et al. (3) demonstrated that the gadolinium concentration measured on electron probe x-ray microanalysis did not increase in regions that were at risk but not infarcted. Fieno et al. (21) showed that image intensities of viable myocardium within the risk region were not elevated compared with the normal myocardium throughout the infarct healing process and irrespective of reperfusion status. There are several factors that potentially affect discrepancies between our findings and the aforementioned papers. In the former, the ischemic period for reversible myocardium (10 or 25 min) and the manner of contrast administration (continuous infusion for 20 min) differed from the present study. In the latter, imaging was performed 30 min after

Figure 3. Corresponding LV Short-Axis Slices of T2W CMR, ECE, and LCE

CMR was performed on day 4 in a patient with anterior myocardial infarction (**A**) and on day 3 in a patient with anterior myocardial infarction (**B**). The epicardium is traced in **green**, endocardium in **red**, and affected region in **yellow**. ECE showed transmural hyperenhancement similar to the areas of increased signal intensity on T2W CMR; whereas, hyperenhanced regions on ECE significantly diminished as compared with those on LCE. CMR = cardiac magnetic resonance; T2W = T2-weighted; other abbreviations as in Figure 1.

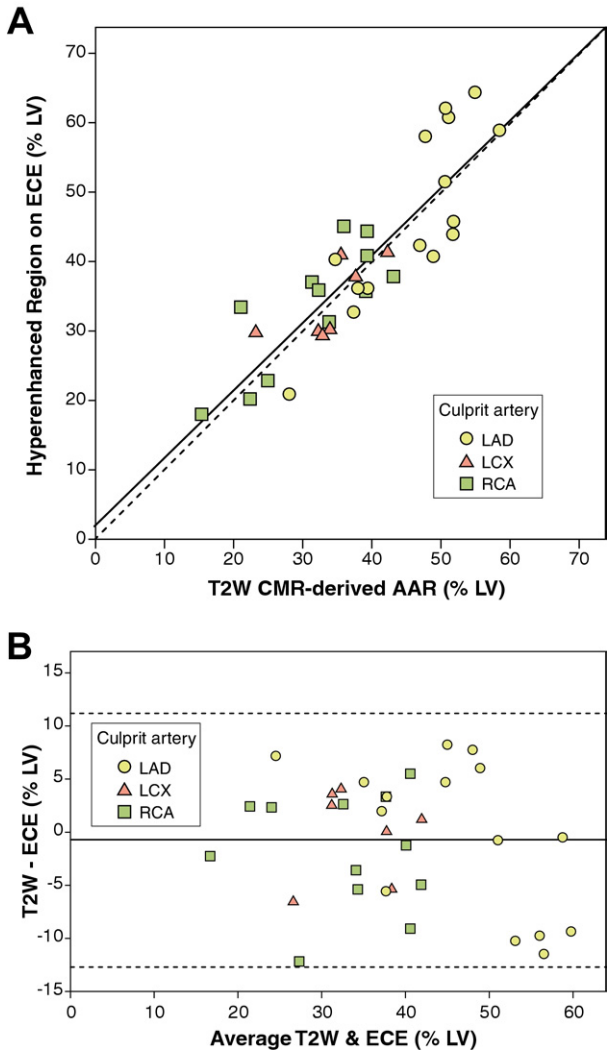

Figure 4. Hyperenhanced Region on ECE and T2W CMR-Derived AAR

(A) Correlation between hyperenhanced region on ECE and T2W CMR-derived AAR ($r = 0.86$, $p < 0.001$). The **solid line** is the regression line, and the **dashed line** is the line of identity. **(B)** Bland-Altman analysis comparing T2W CMR-derived AAR and hyperenhanced region on ECE. The **solid line** is the average difference, and the **dashed lines** represent the bias ±2 SD limits between the 2 measurements. AAR = area at risk; other abbreviations as in Figures 1 and 3.

gadolinium administration. These papers did not address the issues that occur during the earlier phase after gadolinium administration. This might explain, in part, the discrepancies of our findings from the previous reports.

Comparison of ECE with AAR. Recent reports validated that T2W CMR performed after AMI can retrospectively identify the AAR in animal models (12,13) and humans (14). Irreversible injury of ischemic myocardium develops as the widely accepted "wave front phenomenon," which occurs first in the subendocardial myocardium then becoming nearly transmural (22). Accordingly, areas of increased signal intensity on T2W CMR are usually transmural and larger than the hyperenhancement on LCE. In the present study, the transmural hyperenhancement on ECE regardless of transmurality on LCE and the relationship between hyperenhancement area on ECE and T2W CMR-derived AAR were observed. Moreover, in the study population with early reperfusion, which has a positive effect on myocardial salvage, the difference in hyperenhancement area between ECE and LCE is large. These findings support the fact that hyperenhanced regions on ECE demarcate not only infarcted myocardium, but also salvaged myocardium.

Clinical implications. To evaluate the efficacy of therapeutic procedures and drugs for AMI, it is clinically important to measure the size of an infarct, as well as myocardium at risk. Although single-photon emission computed tomography imaging with a technetium perfusion tracer injection prior to acute reperfusion is a widely practiced technique to determine myocardium at risk in humans (23), there are many drawbacks to its widespread use. Recent studies have demonstrated that early imaging after gadolinium administration can be used for detection of microvascular obstruction (24,25). Our findings indicate that ECE using the adjusted TI to null normal myocardium can provide the information on both early microvascular obstruction and AAR. Furthermore, ECE can be acquired during the waiting time for LCE, resulting in reduced examination time for acutely ill patients.

Study limitations. First, the present study was conducted on a relatively small number of patients in limited cohort. Second, the optimal timing for measurement of ECE to demarcate AAR is unknown. Ischemic injury in the peri-infarct zone could be partly restored between reperfusion to CMR. Third, only 3 short-axis slices were acquired so that contrast agent washout effects were minimized during each CE imaging session. Furthermore, our study protocol necessitated T2W imaging and 2 CE imaging sessions, which could be inconvenient for acutely ill patients. In order to improve patient compliance, reduction of the number of slices was applied in this study. Fourth, increased slice thickness was used so that signal-to-noise ratio was improved. T2W imaging using a turbo spin echo readout with dark-blood preparation could be limited by a low signal-to-noise ratio or artifact problems due to the long echo time or through-plane cardiac motion (26,27). In addition,

parallel imaging was employed to speed imaging at the cost of reduced signal-to-noise ratio. Therefore, increased slice thickness was applied to compensate for these limitations. Although partial volume effects could affect the measurement of hyperenhancement, the comparison of hyperenhancement between ECE and LCE using the same slice thickness would support our conclusions. Lastly, T2W imaging was used to determine AAR as a reference. In the absence of a reference standard (e.g., microspheres), these issues are difficult to resolve in the clinical setting.

CONCLUSIONS

This is the first study, to our knowledge, to evaluate peri-infarct zone on ECE using the current standard technique in patients with AMI after reperfusion therapy. Our results suggest that hyperenhanced regions on ECE include the peri-infarct zone, which is ischemically injured but salvaged myocardium. The myocardium at risk and infarcted myocardium after reperfused AMI can be retrospectively assessed by the combination of ECE and LCE using the same imaging sequence.

Reprint requests and correspondence: Dr. Hidenari Matsumoto, Cardiovascular Center, Rakuwakai Otowa Hospital, Kyoto 2, Otowachoinji-cho, Yamashina-ku, Kyoto 607-8062, Japan. *E-mail: matsumoto.hidenari@gmail.com.*

REFERENCES

1. Kim HW, Farzaneh-Far A, Kim RJ. Cardiovascular magnetic resonance in patients with myocardial infarction. Current and emerging applications. J Am Coll Cardiol 2010;55:1–16.
2. Kim RJ, Shah DJ, Judd RM. How we perform delayed enhancement imaging. J Cardiovasc Magn Reson 2003;5:613–5.
3. Rehwald WG, Fieno DS, Chen EL, Kim RJ, Judd RM. Myocardial magnetic resonance imaging contrast agent concentrations after reversible and irreversible ischemic injury. Circulation 2002;105:224–9.
4. Wagner A, Mahrholdt H, Thomson L, et al. Effects of time, dose, and inversion time for acute myocardial infarct size measurements based on magnetic resonance imaging-delayed contrast enhancement. J Am Coll Cardiol 2006;47:2027–33.
5. Kim RJ, Fieno DS, Parrish TB, et al. Relationship of MRI delayed contrast enhancement to irreversible injury, infarct age, and contractile function. Circulation 1999;100:1992–2002.
6. Saeed M, Bremerich J, Wendland MF, Wyttenbach R, Weinmann HJ, Higgins CB. Reperfused myocardial infarction as seen with use of necrosis-specific versus standard extracellular MR contrast media in rats. Radiology 1999;213:247–57.
7. Saeed M, Lund G, Wendland MF, Bremerich J, Weinmann H, Higgins CB. Magnetic resonance characterization of the peri-infarction zone of reperfused myocardial infarction with necrosis-specific and extracellular nonspecific contrast media. Circulation 2001;103:871–6.
8. Judd RM, Lugo-Olivieri CH, Arai M, et al. Physiological basis of myocardial contrast enhancement in fast magnetic resonance imaging of 2-day-old reperfused canine infarct. Circulation 1995;92:1902–10.
9. Schaefer S, Malloy CR, Katz J, et al. Gadolinium-DTPA-enhanced nuclear magnetic resonance imaging of reperfused myocardium: identification of the myocardial bed at risk. J Am Coll Cardiol 1988;12:1064–72.
10. Oshinski JN, Yang Z, Jones JR, Mata JF, French BA. Imaging time after Gd-DTPA injection is critical in using delayed enhancement to determine infarct size accurately with magnetic resonance imaging. Circulation 2001;104:2838–42.
11. Ibrahim T , Nekolla SG, Hörnke M, et al. Quantitative measurement of infarct size by contrast-enhanced magnetic resonance imaging early after acute myocardial infarction: comparison with single-photon emission tomography using Tc99m-sestamibi. J Am Coll Cardiol 2005;45:544–52.
12. Aletras AH, Tilak GS, Natanzon A, et al. Retrospective determination of the area at risk for reperfused acute myocardial infarction with T2-weighted cardiac magnetic resonance imaging: histopathological and displacement encoding with stimulated echoes (DENSE) functional validations. Circulation 2006;113:1865–70.
13. Tilak GS, Hsu L-Y, Hoyt RF, Arai AE, Aletras AH. In vivo T2 weighted magnetic resonance imaging can accurately determine the ischemic area at risk for 2-day-old nonreperfused myocardial infarction. Invest Radiol 2008;43:7–15.
14. Friedrich MG, Abdel-Aty H, Taylor A, Schulz-Menger J, Messroghli D, Dietz R. The salvaged area at risk in reperfused acute myocardial infarction as visualized by cardiovascular magnetic resonance. J Am Coll Cardiol 2008;51:1581–7.
15. Cerqueira MD, Weissman NJ, Dilsizian V, et al. American Heart Association Writing Group on Myocardial Segmentation and Registration for Cardiac Imaging. Standardized myocardial segmentation and nomenclature for tomographic imaging of the heart: a statement for healthcare professionals from the Cardiac Imaging Committee of the Council on Clinical Cardiology of the American Heart Association. Circulation 2002;105:539–42.
16. Judd RM, Kim RJ. Imaging time after Gd-DTPA injection is critical in using delayed enhancement to determine infarct size accurately with magnetic resonance imaging. Circulation 2002;106:e6.
17. Dauber IM, VanBenthuysen KM, Mc-Murtry IF, et al. Functional coronary artery microvascular injury evident as increased permeability due to brief ischemia and reperfusion. Circ Res 1990;66:986–98.
18. Zhao M, Zhang H, Robinson TF, Factor SM, Sonnenblick EH, Eng C. Profound structural alterations of the extracellular collagen matrix in post-ischemic dysfunctional ("stunned") but viable myocardium. J Am Coll Cardiol 1987;10:1322–34.
19. Arheden H, Saeed M, Higgins CB, et al. Reperfused rat myocardium subjected to various durations of ischemia: estimation of the distribution volume of contrast material with echo-planar MR imaging. Radiology 2000;215:520–8.

JACC: CARDIOVASCULAR IMAGING, VOL. 4, NO. 6, 2011
JUNE 2011:610–8

20. Klein C, Schmal TR, Nekolla SG, Schnackenburg B, Fleck E, Nagel E. Mechanism of late gadolinium enhancement in patients with acute myocardial infarction. J Cardiovasc Magn Reson 2007;9:653–8.
21. Fieno DS, Kim RJ, Chen EL, Lomasney JW, Klocke FJ, Judd RM. Contrast-enhanced magnetic resonance imaging of myocardium at risk: distinction between reversible and irreversible injury throughout infarct healing. J Am Coll Cardiol 2000;36:1985–91.
22. Reimer KA, Jennings RB. The "wavefront phenomenon" of myocardial ischemic cell death. II. Transmural progression of necrosis within the framework of ischemic bed size (myocardium at risk) and collateral flow. Lab Invest 1979;40:633–44.
23. Gibbons RJ, Verani MS, Behrenbeck T, et al. Feasibility of tomographic 99mTc-hexakis-2-methoxy-2-methylpropyl-isonitrile imaging for the assessment of myocardial area at risk and the effect of treatment in acute myocardial infarction. Circulation 1989;80:1277–86.
24. Bekkers SC, Backes WH, Kim RJ, et al. Detection and characteristics of microvascular obstruction in reperfused acute myocardial infarction using an optimized protocol for contrast-enhanced cardiovascular magnetic resonance imaging. Eur Radiol 2009;19:2904–12.
25. Nijveldt R, Hofman MB, Hirsch A, et al. Assessment of microvascular obstruction and prediction of short-term remodeling after acute myocardial infarction: cardiac MR imaging study. Radiology 2009;250:363–70.
26. Kellman P, Aletras AH, Mancini C, McVeigh ER, Arai AE. T2-prepared SSFP improves diagnostic confidence in edema imaging in acute myocardial infarction compared to turbo spin echo. Magn Reson Med 2007;57:891–7.
27. Keegan J, Gatehouse PD, Prasad SK, Firmin DN. Improved turbo spin echo imaging of the heart with motion-tracking. J Magn Reson Imaging 2006;24:563–70.

Key Words: acute myocardial infarction ■ area at risk ■ early contrast-enhanced cardiac magnetic resonance ■ late contrast-enhanced cardiac magnetic resonance ■ peri-infarct zone.